

# Testing gravity using the growth of large scale structure in the Universe

E. Jennings<sup>1,2</sup>, C. M. Baugh<sup>1</sup>, S. Pascoli<sup>2</sup>

elise.jennings@durham.ac.uk

*Institute for Computational Cosmology, Department of Physics, Durham University, South Road, Durham, DH1 3LE, U.K.*

*Institute for Particle Physics Phenomenology, Department of Physics, Durham University, South Road, Durham, DH1 3LE, U.K.*

## ABSTRACT

Future galaxy surveys hope to distinguish between the dark energy and modified gravity scenarios for the accelerating expansion of the Universe using the distortion of clustering in redshift space. The aim is to model the form and size of the distortion to infer the rate at which large scale structure grows. We test this hypothesis and assess the performance of current theoretical models for the redshift space distortion using large volume N-body simulations of the gravitational instability process. We simulate competing cosmological models which have identical expansion histories - one is a quintessence dark energy model with a scalar field and the other is a modified gravity model with a time varying gravitational constant - and demonstrate that they do indeed produce different redshift space distortions. This is the first time this approach has been verified using a technique that can follow the growth of structure at the required level of accuracy. Our comparisons show that theoretical models for the redshift space distortion based on linear perturbation theory give a surprisingly poor description of the simulation results. Furthermore, the application of such models can give rise to catastrophic systematic errors leading to incorrect interpretation of the observations. We show that an improved model is able to extract the correct growth rate. Further enhancements to theoretical models of redshift space distortions, calibrated against simulations, are needed to fully exploit the forthcoming high precision clustering measurements.

*Subject headings:* Methods: numerical — Cosmology: theory — dark energy

## 1. Introduction

The accelerating expansion of the Universe can be explained either by a dark energy component or a modification to gravity. In both alternatives, the cosmic expansion history can be described using an effective equation of state,  $w(a)$ , where  $a$  is the scale factor. If two models have the same  $w(a)$ , then, as a consequence, it is not possible to distinguish them using a measurement of the expansion history alone. Structures are, however, expected to collapse under gravity at different rates in dark energy and modified gravity cosmologies. In general relativity, the growth of density perturbations depends only on the expansion history through the Hubble parameter,  $H(a)$ , or equivalently,  $w(a)$  (Linder 2005). This is not the case in modified gravity theories. By using the measured expansion history to predict the growth rate of structure and comparing this estimate to a direct measurement, it has been argued that it is possible to determine the physical origin of the accelerating cosmic expansion (Lue et al. 2004; Linder 2005). If there is no discrepancy between the observed growth rate and the prediction assuming general relativity, this implies that a dark energy component is responsible for the accelerated expansion.

Here we test this hypothesis using large N-body simulations which are the only way to accurately follow the growth of cosmic structure and hence to probe the limits of perturbation theory. Previous simulations of gravitational instability in hierarchical cosmologies have shown that linear theory gives a surprisingly poor description of fluctuation growth and the redshift space distortion of clustering, even on large scales (e.g. Angulo et al. 2008; Smith et al. 2008; Jennings et al. 2010b). We simulate the growth of structure in a modified gravity model and a dark energy model which, by construction, have the same expansion history. The growth rate is measured from the appearance of the power spectrum in redshift space. The goals of this paper are, firstly, to determine if these competing cosmologies can be distinguished from the distortion of clustering as measured in redshift space, using the simulation results, and secondly, to test theoretical models of the power spectrum in redshift space against the simulation results, to assess how well they can recover the growth rate.

This letter is set out as follows. In Section 2 we review the growth of perturbations and describe the modified gravity model. Clustering in redshift space is measured in Section 3, and theoretical models are applied to describe the simulation results. In Section 4 we present our conclusions.

## 2. The cosmological models and simulations

Here we recap how perturbation growth depends on the expansion history and the strength of gravity (Section 2.1), before outlining the modified gravity model (Section 2.2) and our N-body simulations (Section 2.3).

### 2.1. The linear growth rate

In the framework of general relativity (GR), the growth of a density fluctuation,  $\delta \equiv (\rho(x, t) - \bar{\rho}_m)/\bar{\rho}_m$ , where  $\bar{\rho}_m$  is the average matter density, depends only on the expansion history,  $H(a)$ . Using the perturbed equations of motion, within GR, the growth of perturbations follows

$$\ddot{\delta} + 2H\dot{\delta} - 4\pi G_N \rho_m \delta = 0, \quad (1)$$

where  $G_N$  is the present gravitational constant found in laboratory experiments and a dot denotes a time derivative. The growth rate is  $f \equiv d\ln\delta/d\ln a$ , where  $\delta(a)$  is the growing mode solution to Eq. 1. Changing variables to  $g \equiv \delta/a$  and allowing the gravitational constant to vary in time, denoted by  $\tilde{G}$ , gives (Linder 2005)

$$\begin{aligned} \frac{d^2 g}{da^2} + \left(5 + \frac{1}{2} \frac{d\ln H^2}{d\ln a}\right) \frac{1}{a} \frac{dg}{da} \\ + \left(3 + \frac{1}{2} \frac{d\ln H^2}{d\ln a} - \frac{3}{2} \frac{\tilde{G}(a)}{G_N} \Omega_m(a)\right) g = 0, \end{aligned} \quad (2)$$

where  $\Omega_m(a)$  is the matter density parameter. Eq. 2 shows that in GR,  $\tilde{G}(a)/G_N = 1$  and the growth of perturbations depends only on the expansion history,  $H(a)$ . In modified gravity theories, however, the growth of perturbations depends on both  $H(a)$  and  $\tilde{G}(a)$ .

### 2.2. Time variation of Newton’s constant

Modifications to GR provide an alternative explanation to dark energy for the accelerating cosmic expansion. Modified gravity theories can generally be divided into models which introduce a new scalar degree of freedom to Einstein’s equations, e.g. scalar tensor or  $f(R)$  theories, and those which change dimensionality of space, e.g. braneworld gravity. In many such models, the time variation of fundamental constants, such as Newton’s gravitational constant,  $G_N$ , is naturally present.

Self consistent scalar tensor theories are viable alternatives to GR and give rise to an accelerating expansion at late epochs. We refer to these as ‘extended quintessence’ models. Calculations which follow spatial variations in the scalar field have shown that, in practice, a broad range of these models can be effectively described with a time varying Newton’s constant (Pettorino & Baccigalupi 2008; Li et al. 2010).

The variation of  $G_N$  is constrained by various observations, such as the lifespan of stars (Teller 1948), the age of globular clusters (degl’Innocenti et al. 1996), the mass of neutron stars (Thorsett 1996) and the synthesis of light nuclei (Umezu et al. 2005; Clifton et al. 2005). A time-varying  $G_N$  would also modify the temperature fluctuations in the cosmic microwave background, shifting the peaks to larger (smaller) scales on increasing (decreasing)  $G_N$ . This leads to a constraint on the variation of  $G$ ,  $\dot{G}/G = (-9.6 \sim 8.1) \times 10^{-12} \text{ yr}^{-1}$  (Chan & Chu 2007).

Here we consider a simple model for  $\tilde{G}$  (Zahn & Zaldarriaga 2003; Umezu et al. 2005; Chan & Chu 2007),

$$\tilde{G} = \mu^2 G_N, \quad (3)$$

where

$$\mu^2 = \begin{cases} \mu_0^2 & \text{if } a < a_* \\ 1 - \frac{a_s - a}{a_s - a_*} (1 - \mu_0^2) & \text{if } a_* \leq a \leq a_s \\ 1 & \text{if } a > a_s. \end{cases} \quad (4)$$

This parametrization describes a smoothly varying  $\tilde{G}$  which converges slowly to its present value,  $G_N$ , and is more physical than those based on step functions (e.g. Cui et al. 2010). The parameter,  $a_*$ , denotes the scale-factor of photon decoupling and the parameters  $\mu_0$  and  $a_s$  quantify the deviation of  $\tilde{G}$  from the laboratory measured value,  $G_N$ , and the scale factor at which  $\tilde{G}$  and  $G_N$  are equal, respectively. The background evolution is given by

$$H^2 = H_0^2 \frac{\tilde{G}}{G_N} \left( \frac{\Omega_m}{a^3} + \Omega_{\text{DE}} e^{3 \int_a^1 \text{dln} a' [1+w(a')]} \right). \quad (5)$$

Note we assume an equation of state  $w(a) = -1$  in the modified gravity model to match  $\Lambda$ CDM. In Eq. 5,  $\Omega_{\text{DE}}$  is the ratio of the dark energy density to the critical density today. In the left panel of Fig. 1, we plot the ratio of the Hubble rate for two different cosmological models with varying  $\tilde{G}$ , to the Hubble rate in a  $\Lambda$ CDM cosmology as a function of redshift. We chose to simulate the model with the maximum deviation of  $\tilde{G}$  from  $G_N$  which is still compatible with CMB measurements and solar system constraints ( $\tilde{G} \rightarrow G$  as  $a \rightarrow 1$ ), which occurs for a stabilization redshift corresponding to  $a_s = 1$  (i.e. the green dot dashed line in Fig. 1).

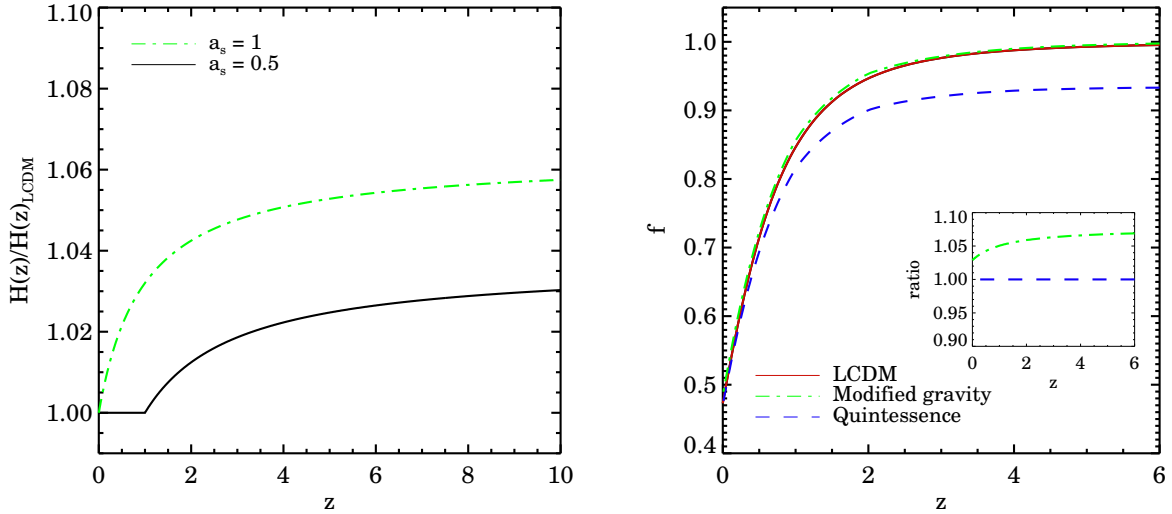


Fig. 1.— Left: Ratio of the expansion rate,  $H(z)$ , to that in  $\Lambda$ CDM for two modified gravity models specified by Eq. 4: dot dashed green line:  $a_s = 1, \mu_0^2 = 1.13$  and solid black line :  $a_s = 0.5, \mu_0^2 = 1.075$ . Right: The linear growth rate,  $f$ , as a function of redshift for  $\Lambda$ CDM (red solid), a modified gravity cosmology with  $a_s = 1$  and  $\mu_0^2 = 1.13$  (green dot dashed) and a quintessence model (blue dashed) with the same expansion history as the modified gravity model. The inset shows the ratio of  $f$  in the modified gravity model to that in the quintessence model as a function of redshift (green dot dashed line).

### 2.3. N-body simulations

We use large volume N-body simulations to carry out the first direct test of the idea that dark energy and modified gravity cosmologies which, by construction, have exactly the same expansion history, can be distinguished by a measurement of the rate at which structure grows. The modified gravity model we simulate has the maximum deviation from Newton’s constant that is compatible with observational constraints, as discussed above. We construct a quintessence model by fitting the expansion history to match the varying  $\tilde{G}$  model within 0.25% over  $0 \leq z \leq 200$ . This model is consistent with constraints on dynamical dark energy (Komatsu et al. 2009; Sánchez et al. 2009).

The simulations were carried out using a memory efficient version of the TreePM code **Gadget-2**, called **L-Gadget-2** (Springel 2005). The simulation used  $N = 1024^3 \sim 1 \times 10^9$  particles in a box of comoving length  $1500h^{-1}\text{Mpc}$ . The comoving softening length was  $\epsilon = 50h^{-1}\text{kpc}$  and the present day linear rms fluctuation in spheres of radius  $8 h^{-1} \text{ Mpc}$  is  $\sigma_8 = 0.8$ . Simulations of extended quintessence cosmologies need to account for both the gravitational correction due to a varying  $\tilde{G}$  in the Poisson equation and a modified expansion history (see Pettorino & Baccigalupi 2008). In the modified gravity simulation, both the long and short-range TreePM algorithm force computations are modified to include a time-dependent gravitational constant. In both the dark energy and modified gravity simulations the Hubble parameter computed by the code was also changed as in Jennings et al. (2010a).

The linear theory power spectrum used to generate the initial conditions was obtained using CAMB (Lewis & Bridle 2002). We adopt a  $\Lambda\text{CDM}$  linear theory power spectrum at  $z = 0$ , and use consistent linear growth factors in each cosmology to obtain the power spectrum amplitude at  $z = 200$ . In principle, as the quintessence cosmology could be classed as an early dark energy model, the linear theory spectrum should be modified in shape. However, as we have shown, such a change has a negligible impact on the nonlinear spectrum and on the ratio of the quadrupole to monopole moments (Jennings et al. 2010a,b).

To obtain errors on our measurements we ran 10 lower resolution simulations with  $512^3$  particles, also in a box of comoving length  $1500h^{-1}\text{Mpc}$ , with different realizations of the density field. The power spectrum was computed using the cloud in cell (CIC) assignment scheme and performing a fast Fourier transform. For the initial conditions the linear growth rate for each model and  $\Lambda\text{CDM}$  was obtained by solving Eq. 2 numerically and is plotted in the right hand panel of Fig. 1 as a function of redshift. For all the models we used the following cosmological parameters:  $\Omega_{\text{m}} = 0.26$ ,  $\Omega_{\text{DE}} = 0.74$ ,  $\Omega_{\text{b}} = 0.044$ ,  $h_0 = H_0/100\text{km s}^{-1}\text{Mpc}^{-1} = 0.715$  and a spectral index of  $n_{\text{s}} = 0.96$  (Sánchez et al. 2009). We have verified that our modifications to Gadget-2 are accurate by checking that the growth of the fundamental mode in the simulations agrees with the linear theory predictions.

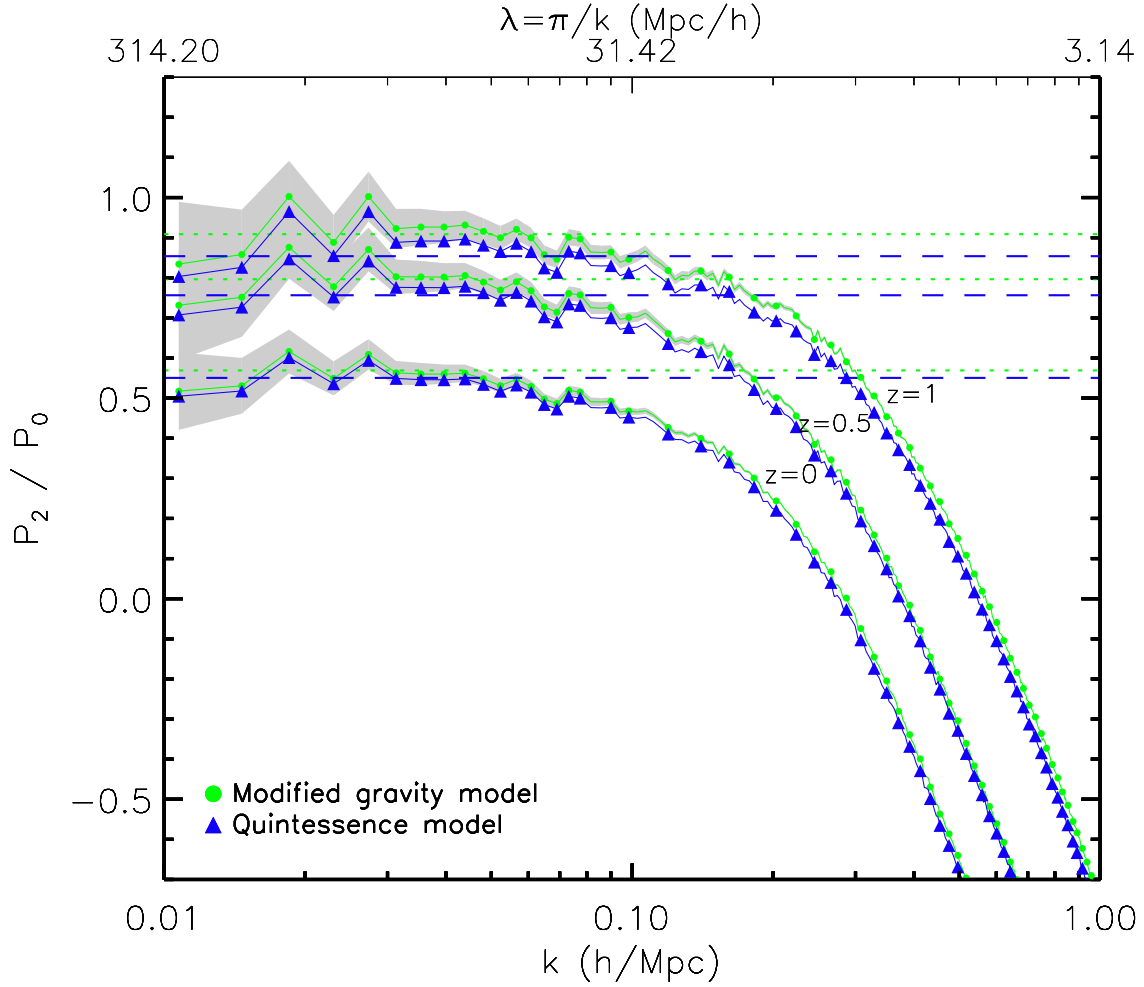


Fig. 2.— The ratio of the quadrupole and monopole moments of the redshift space power spectrum,  $P_2/P_0$ , as a function of wavenumber at redshifts  $z = 0, 0.5$  and  $1$  (in order of ascending amplitude). The points show the N-body results, for the modified gravity model (green triangles) and the quintessence model (blue circles). The shading indicates the error on the ratio, estimated from the scatter over 10 lower resolution simulations. The horizontal lines show the predictions of linear theory model, with the colours having the same meaning as those used for the points.

### 3. Results

We now briefly recap the models used to describe the redshift space distortion of the matter power spectrum and then (S 3.2) fit these models to the moments of the power spectrum measured in our simulations.

#### 3.1. Redshift space distortions

The matter power spectrum in redshift space can be decomposed into multipole moments using Legendre polynomials. The ratio of the quadrupole and monopole moments of the matter power spectrum is plotted in Fig. 2. We model redshift space distortions in the distant observer approximation by perturbing the particle positions down one of the cartesian axes, using the suitably scaled component of the peculiar velocity. The simulation results show that this ratio has a strong dependence on wavenumber. This can be contrasted with the linear perturbation theory prediction (Cole et al. 1994),

$$\frac{P_2(k)}{P_0(k)} = \frac{4\beta/3 + 4\beta^2/7}{1 + 2\beta/3 + \beta^2/5}, \quad (6)$$

where  $\beta = f/b$  and  $b$  is the linear bias, which is unity for dark matter; Eq. 6 is independent of scale (horizontal lines in Fig. 2). We note that, by considering redshift space distortions in the clustering of the dark matter, we are testing theoretical models against the simplest possible case. The distortions will inevitably be more complicated for dark matter haloes and galaxies, for which the bias factor  $b$  can have scale dependence (e.g. Angulo et al. 2008).

In Fig. 2 the quadrupole to monopole ratio increases in amplitude with redshift, due to the evolution in the matter density parameter. At  $z = 0$  there is a 2.5% difference between the linear theory growth rates in the two models. However, at this level, the measured ratios  $P_2/P_0$  are indistinguishable on the very largest scales  $k < 0.02h/\text{Mpc}$  (green dotted and blue dashed horizontal lines). At  $z = 0.5$  and  $z = 1$  the linear theory predictions for the growth rates in the two models differ by 4% and 6% respectively. The error on this ratio measured from the lower resolution simulations is shown by the shaded region in Fig. 2.

In addition to the linear theory model we consider two variants. The first is the Gaussian model (Peacock & Dodds 1994),

$$P^s(k, \mu) = P^r(k)(1 + \beta\mu^2)^2 e^{(-k^2\mu^2\sigma_p^2)}, \quad (7)$$

where  $\sigma_p$  is the pairwise velocity dispersion along the line of sight, which is treated as a parameter to be fitted. We refer to Eq. 7 as the “linear theory plus damping” model. The



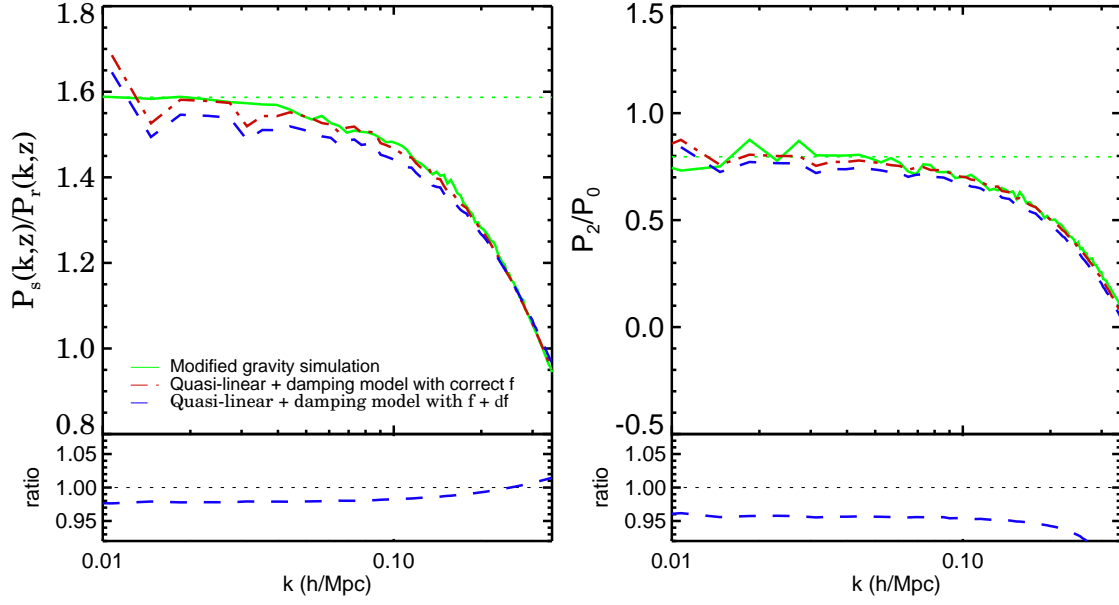


Fig. 3.— Left: The ratio of the monopole of the redshift space power spectrum to the real space  $P(k)$  at  $z = 0.5$ , as a function of wavenumber. Right: The ratio of the quadrupole to monopole moment of the redshift space  $P(k)$ . The quasi-linear plus damping model is plotted using  $f = f_{\text{true}}$  ( $f = 1.05f_{\text{true}}$ ) as a red dot dashed (blue dashed) line. The lower panels show the ratio of  $P_0^s/P_r$  (right:  $P_2^s/P_0^s$ ) using  $f = 1.05f_{\text{true}}$  to the same model using  $f = f_{\text{true}}$  (blue dashed line).

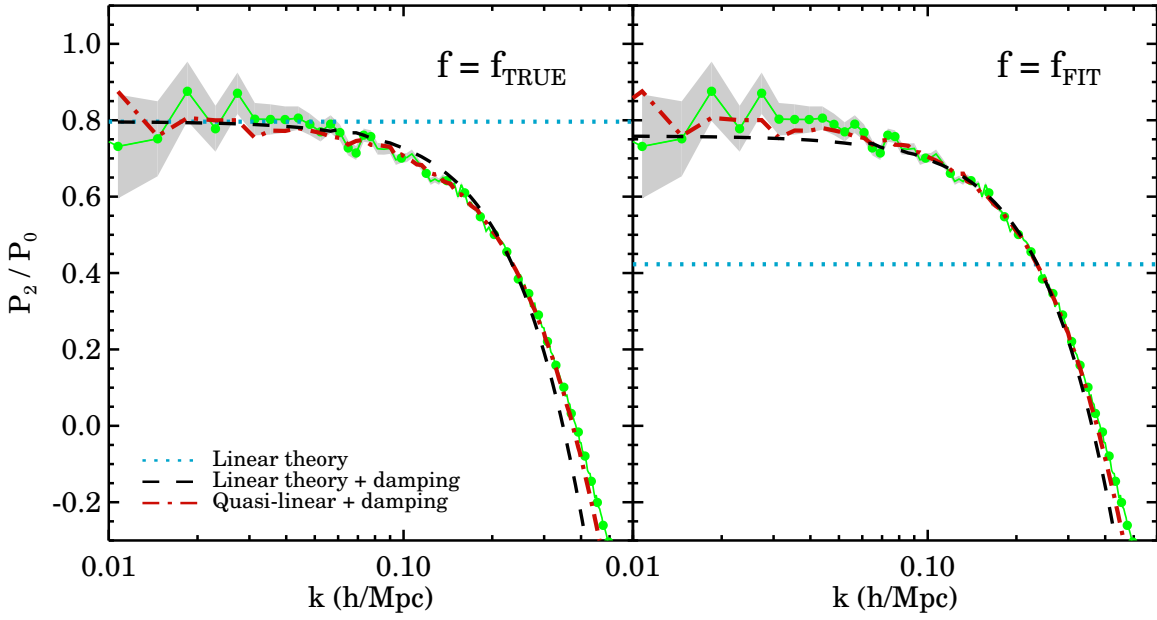


Fig. 4.— The ratio  $P_2/P_0$  in the modified gravity cosmology measured from the high resolution simulation (green points), together with three models for  $P_2/P_0$ , using the correct linear growth rate,  $f = f_{\text{TRUE}}$  (left), and the value of  $f$  obtained in a  $\chi^2$  fit over the wavenumber range  $0.01 \leq k(h/\text{Mpc}) \leq 0.25$ ,  $f = f_{\text{FIT}}$  (right). The shaded region shows the propagated errors from ten lower resolution simulations. The models plotted are indicated by the key: linear theory - blue dotted line, linear theory plus damping - black dashed line and quasi-linear plus damping - red dashed line. In the left panel the best fit value for  $\sigma_p$  ( $\sigma_v$ ) obtained in the range  $0.01 \leq k(h/\text{Mpc}) \leq 0.25$ , with fixed  $f$ , was used for the linear theory plus damping (quasi-linear plus damping) model.

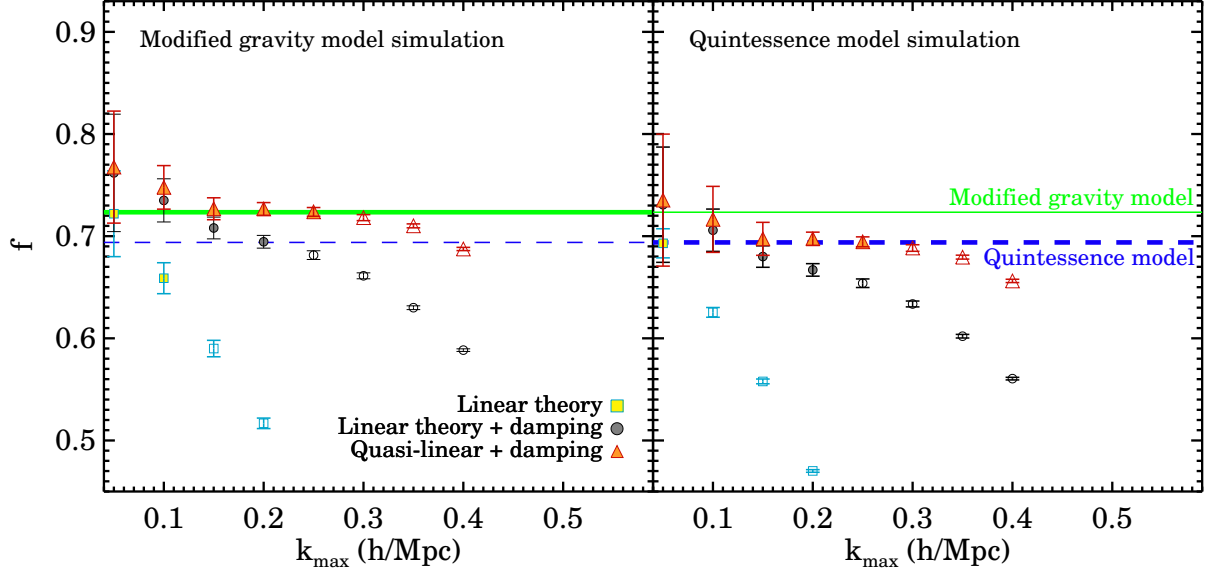


Fig. 5.— Measurements of the growth rate  $f$ . The results are plotted as a function of the maximum wavenumber used in the fit,  $k_{\text{max}}(h/\text{Mpc})$ . The symbols show the results of fitting to  $P_2/P_0$  at  $z = 0.5$  using different models: linear theory - squares, linear theory plus damping - circles, quasi-linear plus damping - triangles. The symbols are filled on scales where the model is a good description of the measured ratio. The error bars represent the  $1\sigma$  uncertainty. Left: we fit to the modified gravity model and aim to recover the true growth factor shown by the thick green horizontal line. Right: we fit to the quintessence model, with the target growth factor shown by the thick blue dashed line.

damping introduces a scale dependence into the ratio  $P_2/P_0$ . The second variant model takes into account departures from linear theory, as well as including small scale damping (Scoccimarro 2004):

$$P^s(k, \mu) = (P_{\delta\delta}(k) + 2f\mu^2 P_{\delta\theta}(k) + f^2\mu^4 P_{\theta\theta}(k)) \times e^{-(fk\mu\sigma_v)^2}, \quad (8)$$

where  $\sigma_v$  is the 1D linear velocity dispersion and  $P_{\theta\theta}$  and  $P_{\delta\theta}$  are the velocity divergence auto and cross power spectrum respectively measured from the simulations (see also Jennings et al. 2010b). We refer to Eq. 8 as the “quasi-linear plus damping” model. We note that  $P_2/P_0$  is more sensitive to changes in  $f$  than the ratio of the monopole moment of the redshift space to real space  $P(k)$ , see Fig. 3, and, as a result, the  $1\sigma$  errors for  $f$  are smaller when fitting to  $P_2/P_0$ .

### 3.2. Measuring the growth rate

We now apply the above models to the simulation results. In Fig. 4, we plot the measured ratio  $P_2/P_0$ , for the modified gravity simulation at  $z = 0.5$ , together with the theoretical predictions. In the left panel, the correct value of  $f$  for this cosmology together with the best fit value for  $\sigma_p$  and  $\sigma_v$  in the range  $0.01 \leq k(h/\text{Mpc}) \leq 0.25$  was used in the linear theory plus damping and quasi-linear plus damping models respectively. In the right panel, the best fit value for  $f$  obtained by fitting over the same range of wavenumbers is used for all models plotted. The value of  $f$  obtained for the linear theory model is sensitive to the maximum value of  $k$  used in the fit. It is clear that both the linear theory and the linear theory plus damping models fail to predict the correct value for  $f$ , with the best fitting values differing by  $\sim 40\%$  and  $\sim 6\%$  respectively from the true value, see Fig. 5. All the models plotted in the right panel in Fig. 4 use the value of  $f$  recovered when  $k_{\text{max}} = 0.25h/\text{Mpc}$ . The quasi-linear plus damping model recovers the correct value of  $f$  over this wavenumber range to within  $\sim 0.64\%$ .

To test these models for the redshift space power spectrum further we vary the maximum wavenumber,  $k_{\text{max}}$ , used in the fit and plot the recovered growth rate as a function of  $k_{\text{max}}$  in Fig. 5. With an accurate model we would recover the correct value for the growth rate  $f$  and the answer would be independent of the value of  $k_{\text{max}}$  adopted, with the only sensitivity to  $k_{\text{max}}$  being in the error on the growth rate. Fig. 5 shows that the quasi-linear plus damping model comes closest to meeting this ideal. Even this model breaks down beyond  $k_{\text{max}} \sim 0.3h/\text{Mpc}$ , which suggests that the modelling of the small scale velocity dispersion can be improved. Most importantly, this model recovers the correct value for  $f$  and can

distinguish between the two cosmologies. The models based on linear theory perform less well. In fact, the answer depends strongly on the maximum wavenumber used in the fit. In Fig. 5 filled symbols are plotted for scales over which the model is a good description of the measured ratio (i.e.  $\chi^2/\nu \sim 1$ , where  $\nu$  is the number of degrees of freedom).

#### 4. Conclusions

Forthcoming galaxy redshift surveys aim to resolve fundamental questions in cosmology, such as the origin of the accelerating expansion. We have measured redshift space distortions in two simulations with different cosmologies and demonstrated that a modified gravity model, described by a time varying Newton’s constant, and a dark energy model, which have identical expansion histories, have measurably different growth rates. We have tested models for redshift space distortions including commonly used linear theory models. We find that models based on linear theory fail to recover the correct value of the growth rate. A quasi-linear model including non-linear velocity divergence terms is far more accurate and allows us to distinguish between these competing cosmologies.

Even though we consider large scales, there are important departures from linear theory which can only be modelled by N-body simulation (Jennings et al. 2010b). Without such guidance, the application of models based on linear theory could lead to systematic errors of the same order as the difference in  $f$  between competing cosmologies. In this event, such models would give the wrong conclusion about the physics driving the cosmic acceleration. We find that an improved model is able to recover the correct growth factor and hence to tell the models apart. This model can be applied to the measured power spectrum over a wider range of scales than those based on linear theory, making better use of the available data. Our tests show that a further improvement to this model is possible. Nevertheless our results show that with such improved models validated against simulations, the prospects of distinguishing between modified gravity and dark energy using clustering measurements are encouraging.

#### Acknowledgments

EJ acknowledges a fellowship from the European Commission’s Framework Programme 6, through the Marie Curie Early Stage Training project MEST-CT-2005-021074. This work was supported by the Science and Technology Facilities Council.

## REFERENCES

- Angulo R., Baugh C. M., Frenk C. S., Lacey C. G., 2008, MNRAS, 383, 755
- Bertschinger E., Zukin P., 2008, Phys. Rev. D, 78, 024015
- Chan K. C., Chu M., 2007, Phys. Rev. D, 75, 083521
- Chevallier M., Polarski D., 2001, Int. J. Mod. Phys., D10, 213
- Clifton T., Barrow J. D., Scherrer R. J., 2005, Phys. Rev. D, 71, 123526
- Cole S., Fisher K. B., Weinberg D. H., 1994, MNRAS, 267, 785
- Cui W., Zhang P., Yang X., 2010, Phys. Rev. D, 81, 103528
- degl’Innocenti S., Fiorentini G., Raffelt G. G., Ricci B., Weiss A., 1996, A&A, 312, 345
- Jennings E., Baugh C. M., Angulo R. E., Pascoli S., 2010a, MNRAS, 401, 2181
- Jennings E., Baugh C. M., Pascoli S., 2010b, MNRAS, p. 1572
- Komatsu E., et al., 2009, ApJS, 180, 330
- Laszlo I., Bean R., 2008, Phys. Rev. D, 77, 024048
- Lewis A., Bridle S., 2002, Phys. Rev. D, 66, 103511
- Li B., Mota D. F., Barrow J. D., 2010, ArXiv e-prints
- Linder E. V., 2003, Phys. Rev. Lett., 90, 091301
- Linder E. V., 2005, Phys. Rev. D, 72, 043529
- Lue A., Scoccimarro R., Starkman G. D., 2004, Phys. Rev. D, 69, 124015
- Peacock J. A., Dodds S. J., 1994, MNRAS, 267, 1020
- Pettorino V., Baccigalupi C., 2008, Phys. Rev. D, 77, 103003
- Sánchez A. G., Crocce M., Cabré A., Baugh C. M., Gaztañaga E., 2009, MNRAS, 400, 1643
- Scoccimarro R., 2004, Phys. Rev. D, 70, 083007
- Smith R. E., Sheth R. K., Scoccimarro R., 2008, Phys. Rev. D, 78, 023523
- Springel V., 2005, MNRAS, 364, 1105

Teller E., 1948, Phys. Rev., 73, 801

Thorsett S. E., 1996, Phys. Rev. Lett., 77, 1432

Umezu K., Ichiki K., Yahiro M., 2005, Phys. Rev. D, 72, 044010

Zahn O., Zaldarriaga M., 2003, Phys. Rev. D, 67, 063002